Kinetics of Enzyme Reactions with Interaction between a Substrate and a (Metal) Modifier*

Wayne P. London and Theodore L. Steck†

ABSTRACT: This study describes a kinetic model of an enzyme reaction in which a (metal) modifier and a reactant combine with the enzyme and with each other. The prototype reaction requires adenosine triphosphate (reactant) and magnesium ion (modifier), the "active substrate" being the magnesium–adenosine triphosphate complex. Sigmoid velocity curves can occur in this model, which does not assume an enzyme with multiple interacting subunits. Qualitative criteria for distinguishing different effects of the modifier and the reactant are: (1) Is a velocity curve concave or sigmoid? (2) What is the relative position of velocity curves obtained with higher fixed concentrations of modifier or reactant? (3) Does a peak velocity occur? (4) What is the position of the peak velocity? (5) How sigmoid is the velocity curve obtained with equal concentrations of modifier and reactant? (6) When either modifier or reactant is in excess is the velocity constant? These criteria help distinguish, for example, inhibition by free reactant (adenosine triphosphate) from activation by free modifier (magnesium). Graphical methods for estimating several kinetic parameters are presented. The methods do not require ths association constant of the modifier–reactant complex (*e.g.*, magnesium–adenosine triphosphate); in some cases that constant can be estimated graphically from the enzyme kinetic data.

Modifiers affect many enzyme reactions by combining with both the enzyme and a reactant. The prototype reaction requires ATP (reactant) and magnesium ion (modifier), the "active substrate" being the Mg–ATP complex (Cleland, 1967). In such systems magnesium and other divalent cations have been observed to exert a complex and perhaps regulatory influence on enzyme activity (*e.g.*, Atkinson *et al.*, 1965; Beck, 1967; Keech and Barritt, 1967; Schramm and Morrison, 1968; Steck *et al.*, 1968).

These reactions are difficult to study because (a) the free modifier and reactant can inhibit the reaction, so that neither can be added in arbitrary excess; and (b) unless the association constant of the modifier–reactant complex, K_0, has been determined, the concentrations of the free modifier, free reactant, and modifier–reactant complex are not known.

If K_0 is known, these concentrations can be calculated, and the reaction can be studied by extensions of classic kinetic techniques (Cleland, 1963; Frieden, 1964; London, 1968). Several ATP–phosphotransferases have been studied in this manner (Morrison *et al.*, 1961; Gaffney and O'Sullivan, 1964; Mildvan and Cohn, 1966). A second approach is to maintain a small fixed excess of free modifier to minimize the often observed inhibition by the free reactant (Cleland, 1967). Both methods require that K_0 be known for the particular experimental conditions under study. Other techniques are to use equal concentrations of modifier and reactant to minimize both free species (Keech and Barritt, 1967), or to hold fixed the total amount of modifier or reactant and vary the other.

This investigation describes a kinetic model and a general method for studying enzyme reactions in which a modifier and a reactant combine with the enzyme and with each other. Procedures are developed for (a) distinguishing different effects of the modifier and the reactant and (b) estimating graphically several kinetic parameters. We first present a general model that defines the problem; then we discuss in detail three special cases of the general model that seem adequate to describe several enzyme reactions.

Assumptions of the General Model

The general model assumes that the enzyme exists in an unmodified and a modified form, and that the modifier and the reactant combine with each other and with the enzyme to form the enzyme–modifier–reactant complex. These reactions are listed in Scheme I. (E is the unmodified enzyme; ME, the modified enzyme; C, the modifier–reactant complex; M, the modifier; and S, the reactant, which is also called the substrate. The K's are association constants and k and k' are rate constants.) The reactions in the first column are the three ways that the modifier, the substrate, and the unmodified enzyme can react to form the EC complex, which yields the products. The reactions in the last column (plus the $M + S \rightleftharpoons C$ reaction) are the three ways that the modifier, the substrate, and the modified enzyme can react to form the MEC complex, which yields the products. The reactions in the second column are the ways that the unmodifier enzyme can be modified. (This modification is usually regarded as activation of the enzyme.)

* From the Mathematical Research Branch, National Institute of Arthritis and Metabolic Diseases and the Chemistry Branch, National Cancer Institute, National Institutes of Health, Bethesda, Maryland 20014. *Received November 12, 1968.*

† Present address: Biochemical Research Laboratory, Massachusetts General Hospital, Boston, Mass. 02114.

SCHEME I

$$\begin{cases} M + S \overset{K_0}{\rightleftharpoons} C \\ E + C \overset{\tilde{K}_C}{\rightleftharpoons} EC \end{cases} \qquad M + E \overset{K_A}{\rightleftharpoons} ME \qquad ME + C \overset{\tilde{K}_{C'}}{\rightleftharpoons} MEC$$

$$\begin{cases} E + S \overset{K_S}{\rightleftharpoons} ES \\ ES + M \overset{K_1}{\rightleftharpoons} EC \end{cases} \qquad M + EM \overset{K_3}{\rightleftharpoons} MEM \qquad \begin{cases} ME + S \overset{K_{S'}}{\rightleftharpoons} MES \\ MES + M \overset{K_{1'}}{\rightleftharpoons} MEC \end{cases}$$

$$M + ES \overset{K_4}{\rightleftharpoons} MES$$

$$\begin{cases} E + M \overset{K_M}{\rightleftharpoons} EM \\ EM + S \overset{K_2}{\rightleftharpoons} EC \end{cases} \qquad M + EC \overset{K_5}{\rightleftharpoons} MEC \qquad \begin{cases} ME + M \overset{K_{M'}}{\rightleftharpoons} MEM \\ MEM + S \overset{K_{2'}}{\rightleftharpoons} MEC \end{cases}$$

$$EC \xrightarrow{k} E + \text{products} \qquad MEC \xrightarrow{k'} ME + \text{products}$$

$$M + S \overset{K_0}{\rightleftharpoons} C$$

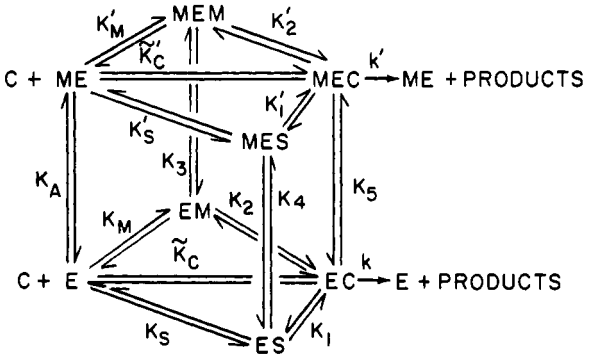

FIGURE 1: The reactions of the general model. The reactions in the horizontal plane are the three ways a final enzyme complex is formed, the lower tier for the unmodified enzyme and the upper tier for the modified enzyme. The vertical reactions are the ways the enzyme is modified. The M and S species are not shown in reactions involving the enzyme. The K's are association constants, and k and k' are rate constants.

The modifier is essential to the reaction.[1] These 17 reactions are shown in Figure 1.

The conservation equations of the system are: $E_t = E + ES + EM + EC + ME + MES + MEM + MEC$, $M_t \cong M_f + C$, and $S_t \cong S_f + C$, where E_t is the total enzyme concentration; M_t and M_f, the concentrations of total and free modifier, respectively; S_t and S_f, the concentrations of total and free substrate, respectively; and C, the concentration of the modifier–substrate complex. (Brackets denoting concentrations are omitted from these and other equations.) These equations assume that M_t and S_t greatly exceed E_t.

The $M + S \rightleftharpoons C$ reaction is assumed to be at equilibrium, so that C is given by the smaller root of

$$C^2 - (M_t + S_t + 1/K_0)C + M_tS_t = 0 \qquad (1)$$

where K_0 is the association constant of the modifier–reactant complex.

We assume that each enzyme species is in the steady state, and, furthermore, that the rates of transitions from one enzyme species to another (including rates of product formation) equal the rates of the reverse transitions. Quasi-equilibrium is a special case of this condition. Under this assumption, which has been discussed by London (1968), the contribution of any particular pathway to the formation of a final enzyme complex cannot be assessed from the steady-state enzyme kinetic data. Each reaction is described by a single kinetic constant, usually an equilibrium constant, and there are equalities among the kinetic constants for reactions around a cycle (Table I; K_C and K_C' are not equilibrium constants). Of the seventeen constants that describe the model, ten are independent. One set of ten constants, from which the others may be derived by means of the relations in Table I, is $\{V, V', K_0, K_S, K_S', K_M, K_M', K_C, K_C', \text{and } K_A\}$.

Under these assumptions the general rate equation for the initial velocity, v, is

$$v = k[EC] + k'[MEC] = \frac{(V + V'K_A(K_C'/K_C)M_f)K_CC}{(K_SS_f + K_MM_f + K_CC + 1) + K_AM_f(K_S'S_f + K_M'M_f + K_C'C + 1)} \qquad (2)$$

Figure 1 and eq 1 and 2 define the problem of enzyme modification where the modifier and a reactant combine with the enzyme and with each other, but for practical use, the model is too general. We shall consider three special cases of this model that are pertinent to many systems.

Model I: an Unmodified Enzyme. The lower tier of reactions in Figure 1 plus the $M + S \rightleftharpoons C$ reaction. If $M_f \gg \bar{K}_A$, this model may be interpreted as the upper tier of reactions, that is, a completely modified enzyme.

Model II. The upper tier of reactions in Figure 1, the $M + S \rightleftharpoons C$ reaction, and the $M + E \rightleftharpoons ME$

[1] A more general model includes product formation from the MES and ES species. If the latter pathway exists there is enzymatic activity without M, since the modifier is not essential to the reaction.

TABLE I: The Kinetic Constants and Relations among the Kinetic Constants.[a]

$K_0 = \frac{(C)}{(M)(S)}$	$V = kE_t$	$V' = k'E_t$
$K_S = \frac{(ES)}{(E)(S)}$	$K_S' = \frac{(MES)}{(ME)(S)}$	$K_A = \frac{(ME)}{(E)(M)}$
$K_M = \frac{(EM)}{(E)(M)}$	$K_M' = \frac{(MEM)}{(ME)(M)}$	$K_3 = \frac{(MEM)}{(EM)(M)}$
K_C[b] $= \frac{(EC)}{(E)(C)}$	$K_C' = \frac{(MEC)}{(ME)(C)}$	$K_4 = \frac{(MES)}{(ES)(M)}$
$K_1 = \frac{(EC)}{(ES)(M)}$	$K_1' = \frac{(MEC)}{(MES)(M)}$	$K_5 = \frac{(MEC)}{(EC)(M)}$
$K_2 = \frac{(EC)}{(EM)(S)}$	$K_2' = \frac{(MEC)}{(MEM)(S)}$	
$K_0K_C = K_MK_2 = K_SK_1$	$K_0K_C' = K_M'K_2' = K_S'K_1'$	
$K_AK_M' = K_3K_M$	$K_AK_S' = K_4K_S$	$K_AK_C' = K_5K_C$

[a] The constants with a prime (*e.g.*, K_S') denote reactions involving the modified enzyme. In subsequent use, $\bar{K} = 1/K$ for all constants. The units of the K's and $\bar{K}$'s are M^{-1} and M, respectively. Association constants rather than dissociation constants are used, so that strong inhibition by the $E + S \rightleftharpoons ES$ reaction, for example, is reflected by a large K_S. [b] K_C and K_C' are Briggs–Haldane constants that include the rate constant of product formation, k or k'. If l_1, l_{-1}, and k are rate constants of

$$E + C \underset{l_{-1}}{\overset{l_1}{\rightleftharpoons}} EC \xrightarrow{k} E + \text{product}$$

then $K_C = l_1/(l_{-1} + k)$ and $1/K_C = l_{-1}/l_1 + k/l_1 = 1/\tilde{K}_C + k/l_1$, where $\tilde{K}_C$ is the association constant $\tilde{K}_C = l_1/l_{-1}$. By analogy, $K_C' = l_1'/(l_{-1}' + k')$ and $1/K_C' = 1/\tilde{K}_C' + k'/l_1'$. The other K's are association constants.

reaction. This is model I plus essential activation of the enzyme.

Model III. A simple model of enzyme modification

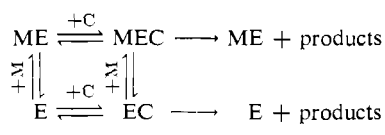

where C, but not S or M, reacts with enzyme to form the final complexes. There are two paths of product formation.

These models do not assume an enzyme with multiple interacting subunits. Although the models assume one substrate, they can be applied to multisubstrate reactions when certain restrictions on the effect of the modifier (Frieden, 1964) are presumed true.

When either S_t or M_t greatly exceeds the other we shall approximate the $M + S \rightleftharpoons C$ reaction and the solution of eq 1 by assuming: if $S_t \gg M_t$: $C \cong M_t$, $S_f \cong S_t - M_t$, and $M_f \cong 0$, or if $M_t \gg S_t$: $C \cong S_t$, $M_f \cong M_t - S_t$, and $S_f \cong 0$. These approximations (which in context are called *the approximation of C*) are increasingly accurate when both M_t and S_t exceed $\bar{K}_0$, that is, in general, when K_0 is large.

Model I

This model assumes that M, S, and C combine with the enzyme to form the final complex. The reactions are

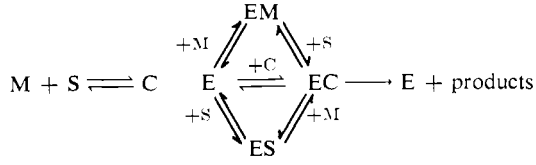

The model has been applied to creatine kinase (Morrison *et al.*, 1961), lombricine kinase (Gaffney and O'Sullivan, 1964), and pyruvate kinase (Mildvan and Cohn, 1966) when K_0 was known.

The rate equation of the model is

$$v = \frac{VK_CC}{K_SS_f + K_MM_f + K_CC + 1} = \frac{VK_CC}{K_SS_t + K_MM_t + (K_C - K_S - K_M)C + 1} \quad (3)$$

(Use of the conservation equations for M_t and S_t in the first version gives the second version.) Since C can be obtained from eq 1, v is a function of two independent variables, M_t and S_t, which are the coordinate axes of the velocity surface. The only asymmetry between S_t and M_t is, in general, K_S does not equal K_M.

A fruitful way to study the velocity surface is to examine profiles obtained by holding one variable fixed and increasing the other. Although we shall usually describe profiles of the velocity surface when M_t is fixed and S_t is increased, analogous results apply when S_t is fixed and M_t is increased. The velocity profile obtained with fixed M_t and increasing S_t is

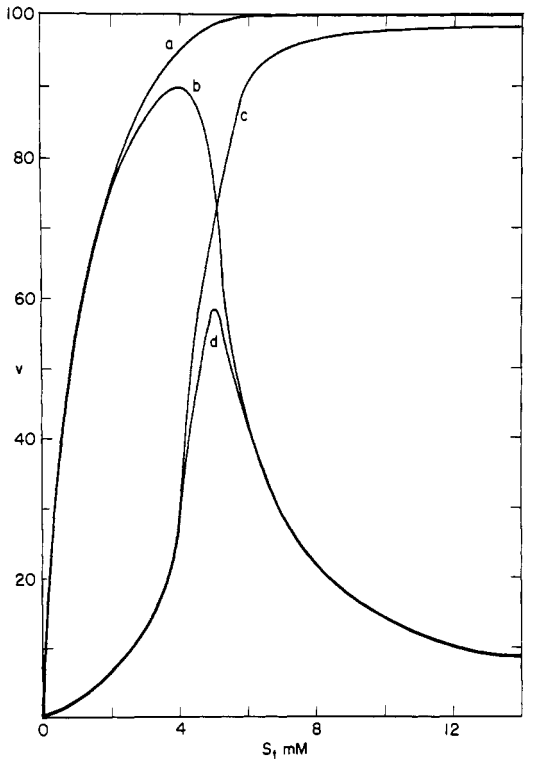

FIGURE 2: The four qualitatively different velocity profiles of model I. For all the profiles $M_t = 5$ mM, $V = 100$, $K_0 = 1 \times 10^5$, and $K_C = 5 \times 10^4$. Profile a is concave with no peak: $K_S = 0$, $K_M = 1 \times 10^4$. Profile b is concave with a peak: $K_S = 3 \times 10^5$, $K_M = 1 \times 10^4$. Profile c is sigmoid with no peak: $K_S = 0$, $K_M = 5 \times 10^5$. Profile d is sigmoid with a peak: $K_S = 3 \times 10^5$, $K_M = 5 \times 10^5$.

called the S_t profile; the profile obtained with fixed S_t and increasing M_t is called the M_t profile. We first discuss qualitative features of model I that depend upon the kinetic constants. Then we present a simulation[2] of the model based on kinetic parameters from the literature in conjunction with two graphical methods to estimate the constants.

This model generates four qualitatively different velocity profiles: the ascending limb limb may be sigmoid or concave[3] and a peak velocity may or may not be present (Figure 2). A peak in Figure 2 implies that $K_S \neq 0$; as S_t is increased the inhibition is from the $E + S \rightleftarrows ES$ reaction. After the peak the velocity asymptotically approaches zero, but if K_S is not large, the slow descent to zero may not be observed.

If the ascending limb of the S_t profile is sigmoid, then $K_M > K_C$. The inhibition is from the $E + M \rightleftarrows EM$ reaction, which is evident when $M_t > S_t$ (so that M_f is relatively abundant). If the ascending limb is concave, then, in general $K_C \geq K_M$. (At low fixed M_t concentrations the ascending limb appears concave even though $K_M > K_C$ (see Appendix). The concavity that occurs when $K_M > K_C$ is easily recognized: it occurs at low fixed M_t concentrations (hence low velocities), and it reverts to the sigmoid shape at higher fixed M_t concentrations.) As noted above, analogous results for M_t profiles are obtained by replacing S_t by M_t and K_S by K_M in the above discussion.[4]

Simulations of model I were done using kinetic constants obtained for the enzyme, lombricine kinase (Gaffney and O'Sullivan, 1964); families of S_t and M_t profiles are shown in Figure 3. In Figure 3a the ascending limb of an S_t profile is sigmoid since $K_M > K_C$ (and the M_t concentration is not low). The curved arrow shows the relative position of the ascending limb of profiles obtained with higher fixed M_t concentrations. (If K_C had exceeded K_M, the ascending limb would have been concave, but, in general, the arrow would still point downward. If $K_M = 0$ the arrow would have pointed upward, since there would be no inhibition by the $E + M \rightleftarrows EM$ reaction.) The profiles show a peak because $K_S \neq 0$. Analogous results apply to the M_t profiles in Figure 3b.

We next show how the S_t and M_t profiles can be used to estimate graphically several kinetic constants; further description of the model is resumed in the section on peak velocities.

Estimation of K_S, K_M, K_C, and V. ISOVELOCITY METHOD. One graphical method to determine K_S, K_M, K_C, and V uses points of equal velocity from families of S_t and M_t profiles. The dashed horizontal lines in Figure 3a,b connect points of equal velocity for $v = 5$, 10, and 20. These *isovelocity* data are replotted with M_t and S_t as the coordinate axes in Figure 3c. The plots are curvilinear in the region near $M_t = S_t$, but when $S_t \gg M_t$ or $M_t \gg S_t$ they are asymptotically linear. When $S_t \gg M_t$, *the approximation of C* may be used in eq 3, and the isovelocity curves are then described by

$$v_i = \frac{VK_CM_t}{1 + K_S(S_t - M_t) + K_CM_t} = \frac{VM_t}{\bar{K}_C(1 + K_S(S_t - M_t)) + M_t} \quad (4a)$$

or

$$v_iS_t + \bar{K}_Sv_i - [v_i + (V - v_i)K_C\bar{K}_S]M_t = 0 \quad (4b)$$

where v_i is a particular observed velocity. From eq 4b the asymptotically linear portion of every isovelocity curve intersects the S_t axis at $-\bar{K}_S$, from which K_S is obtained directly. The slope of the asymptotically linear portion is

$$\frac{dS_t}{dM_t} = (1 - K_C\bar{K}_S) + VK_C\bar{K}_S(1/v_i) \quad (5)$$

[2] All simulations were done with programs written in FORTRAN for the UNIVAC 1108 computer.

[3] We use *concave* to describe a curve with a decreasing slope. Thus, the hyperbola of Michaelis–Menten kinetics is concave.

[4] The results concerning the concavity and sigmoidicity of the ascending limb of the S_t profile are based on the sign of the second derivative in a neighborhood of $S_t = 0$. The possibility of the profile having two inflection points before the peak (*e.g.*, initially concave and then sigmoid) can be excluded when $K_S = 0$, but the proof appears intractable in the general case. Numerous simulations tend to exclude this possibility with model I, but the phenomenon is readily observed with model III. We conjecture that a curve with two inflection points and no intervening extremum implies multiple paths of product formation.

Once K_S is known, V and K_C can be estimated from a plot of dS_t/dM_t *vs.* $1/v_i$ in eq 5.

The analogous equations for $M_t \gg S_t$ are

$$v_i = \frac{VK_CS_t}{1 + K_M(M_t - S_t) + K_CS_t} = \frac{VS_t}{\bar{K}_C(1 + K_M(M_t - S_t) + S_t} \quad (6a)$$

or

$$v_iM_t + \bar{K}_Mv_i - [v_i + (V - v_i)K_C\bar{K}_M]S_t = 0 \quad (6b)$$

In eq 6b the intercept of the M_t axis is $-\bar{K}_M$, and the slope is

$$\frac{dM_t}{dS_t} = (1 - K_C\bar{K}_M) + VK_C\bar{K}_M(1/v_i) \quad (7)$$

Once K_M is obtained from the intercept on the M_t axis in eq 6b, V and K_C can be estimated from a plot of dM_t/dS_t *vs.* $1/v_i$ in eq 7. These procedures are illustrated in Figure 3c–e for the lombricine kinase simulation.

These graphical procedures depend upon *the approximation of C*, which is increasingly accurate when S_t greatly exceeds M_t or *vice versa*. Thus, K_S is estimated when S_f is abundant ($S_t \gg M_t$), and K_M is estimated when M_f is abundant ($M_t \gg S_t$). More accurate estimations are obtained from low isovelocities. (The isovelocities in Figure 3c are 15–60% of the observed peak velocity.) In these procedures the isovelocities from the $S_t \gg M_t$ and the $M_t \gg S_t$ regions need not be the same.

The intercepts in Figure 3c overestimate the reciprocals of the kinetic constants (underestimate K_S or K_M). If K_S is large relative to K_0 or K_C, as in Figure 3c, this overestimation is appreciable. To minimize this error, the intercepts may be extrapolated to zero isovelocity to obtain a more accurate estimation of $\bar{K}_S$, as illustrated in the inset of Figure 3c. This extrapolation has the effect of utilizing low isovelocities that would come from a region where *the approximation of C* is more accurate. In contrast, the estimation of K_M in Figure 3c is accurate without the replot of the intercepts. If K_S or K_M is large, so that $\bar{K}_S$ and $\bar{K}_M$ is small relative to $\bar{K}_0$, to $\bar{K}_C$, and to the S_t or M_t concentration range, then the intercept is near zero, and the constant is difficult to estimate accurately. Because of the redundancy of estimating V and K_C from regions of $S_t \gg M_t$ and $M_t \gg S_t$, V and K_C can be found from the more accurately determined of K_S or K_M. Then they can be used to obtain the less accurately determined of K_S or K_M by substitution into eq 5 or 7.

FIXED EXCESS METHOD. A second graphical method to estimate K_S, K_M, K_C, and V uses eq 4a and 6a. If velocity data are obtained in the region $S_t \gg M_t$ so that a *fixed excess* of S_t over M_t is maintained, then eq 4a is of the Michaelis–Menten form. The maximal velocity, V, and an apparent kinetic constant, $\bar{K}_{C,app} = \bar{K}_C(1 + K_S(S_t - M_t))$, are estimated from classic double-reciprocal plots. A plot of $\bar{K}_{C,app}$ *vs.* the different fixed excesses, $S_t - M_t$, has intercept $\bar{K}_C$ and slope $\bar{K}_CK_S$. By analogy, in the region $M_t \gg S_t$, K_M, K_C, and V can be estimated from eq 6a by the fixed excess method. These procedures are illustrated in Figure 3f,g for the lombricine kinase simulation. The fixed excess method has the same redundancy in estimating V and K_C as the isovelocity method.

The use of a fixed excess of metal ion (usually 1 mM) to minimize inhibition by S in the determination of $\bar{K}_C$ has been advocated (Cleland, 1967; Gulbinsky and Cleland, 1968; Morrison and James, 1965). From 6a (and Figure 3g) the kinetic constant determined by this fixed excess method is $\bar{K}_C(1 + K_M(M_t - S_t))$ and not $\bar{K}_C$. At a fixed excess of metal of 1 mM the error can be significant. (For example, if $K_M = 1 \times 10^4$, the error is 11-fold.)

It is difficult to assess any advantage of the isovelocity method over the fixed excess method in obtaining K_S, K_M, K_C, and V. Both techniques depend upon *the approximation of C*, and, in general, both are difficult to apply if K_S or K_M is large relative to K_0 or K_C. The isovelocity method uses interpolations between data points, and not all data points are used; this method requires one more graphical step than the other, and perhaps a final extrapolation. The fixed excess method gives convergent linear plots even when the procedure does not accurately estimate the kinetic constants, and the experimental design is slightly more complex.

We now discuss the locus of peak velocities, which is used to determine K_0 and, as will be shown, to help distinguish model I and model II.

LOCUS OF PEAK VELOCITIES AND THE ESTIMATION OF K_0. If $K_S \neq 0$ the S_t profiles show a peak velocity, and if $K_M \neq 0$ the M_t profiles show a peak velocity. The location of the peak in the S_t profile depends upon M_t and *vice versa* (the equations appear in the Appendix). For the simulation of lombricine kinase the loci of peak velocities as a function of S_t and M_t are plotted in Figure 3h. (The locus of peaks from the S_t profiles is called the S_t *locus*, and the M_t *locus* is from the M_t profiles.)

The peak does not occur when the ratio of M_t to S_t is one to one; instead the location depends upon the relation of K_M to K_S. If $K_S > K_M$, as in Figure 3h, the M_t locus occurs where M_t exceeds S_t. The smaller K_0, the larger the excess. The S_t locus in Figure 3h occurs in the region where $S_t > M_t$ at very low M_t concentrations, but at higher M_t concentrations the peak occurs where M_t exceeds S_t. Analogous results apply if $K_M > K_S$. The loci of peaks are independent of V and K_C; they depend only upon K_S, K_M, and K_0. In general, the loci are nonlinear. Other characteristics of the loci of the peak velocities appear in the Appendix.

The S_t locus intersects the S_t axis at $S_t = \sqrt{\bar{K}_S\bar{K}_0}$, and the M_t locus intersects the M_t axis at $M_t = \sqrt{\bar{K}_M\bar{K}_0}$. Once K_S or K_M is known, K_0 can be found from the appropriate intercept[5] (Figure 3h).

[5] Once K_M (or K_S) and K_0 are known, a large K_S (or K_M), difficulty to estimate by the isovelocity or fixed excess methods, conceivably could be estimated from these intercepts.

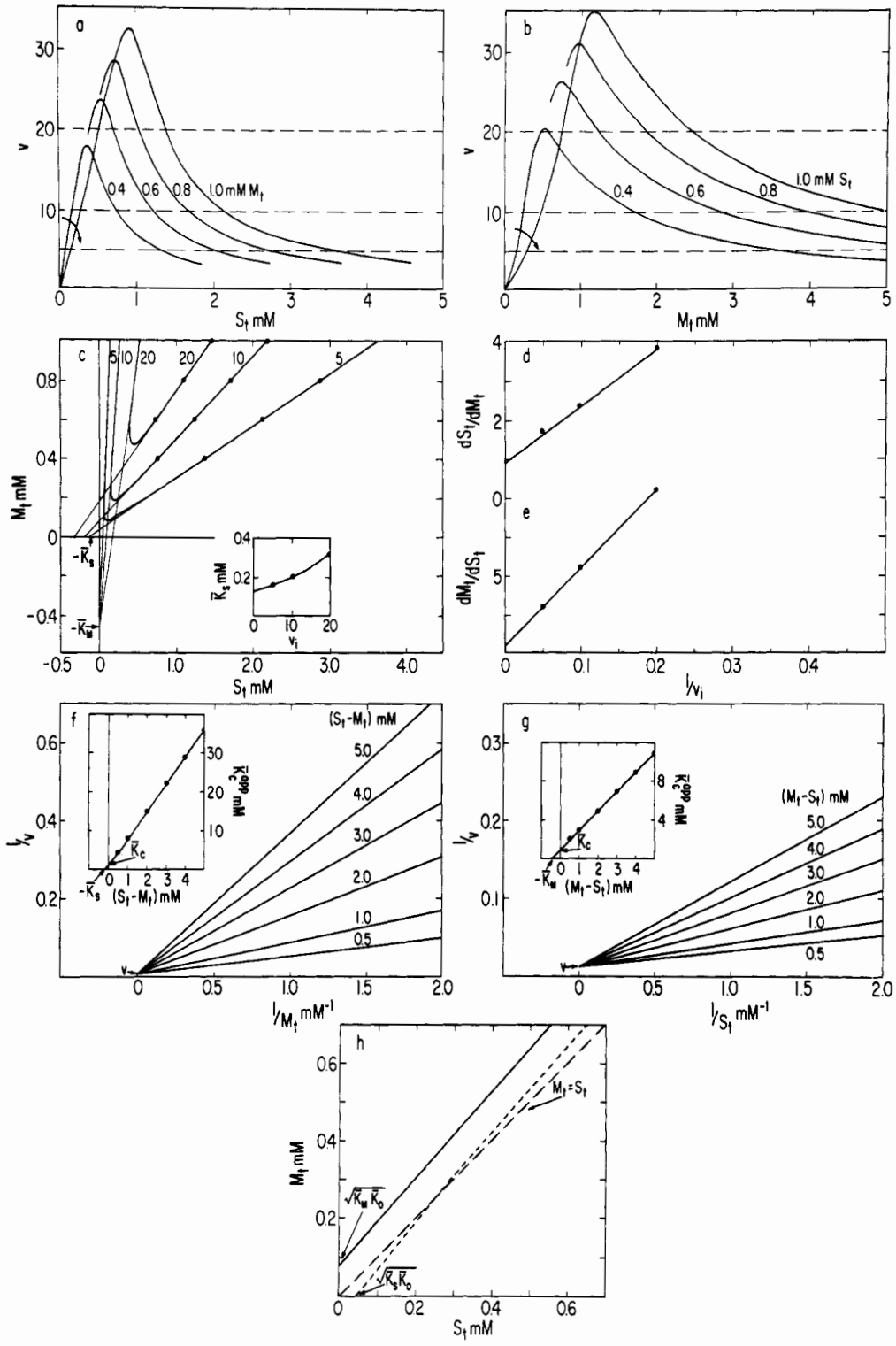

If both K_S and K_M are known, K_0 can also be obtained from single observations of the location of the peak velocity and the quadratic expression

$$\bar{K}_0^2 + (2M_t - Q - S_t^2/Q)\bar{K}_0 + (M_t - S_t)^2 = 0 \quad (8)$$

where $Q = \bar{K}_S(K_M M_t + 1)$ and S_t and M_t are the coordinates of the peak.[6]

[6] Equation 8, a rearrangement of eq A-2 in the Appendix, describes the S_t locus of peak velocities. The analogous equation for the M_t locus is obtained from eq 8 by replacing K_S by K_M and S_t by M_t. In general, K_0 is the smaller root of eq 8. If the locus crosses the $M_t = S_t$ line, the larger root is chosen at very low M_t concentrations until the discriminant vanishes, and then the smaller root is chosen.

FIGURE 3: Simulation and analysis of data of model I. The kinetic parameters are from the lombricine kinase reaction (Gaffney and O'Sullivan, 1964): $V = 100$, $K_0 = 7.14 \times 10^4$ ($\bar{K}_0 = 1.4 \times 10^{-5}$), $K_C = 1.11 \times 10^3$ ($\bar{K}_C = 9 \times 10^{-4}$), $K_S = 7.69 \times 10^3$ ($\bar{K}_S = 1.3 \times 10^{-4}$), $K_M = 2.22 \times 10^3$ ($\bar{K}_M = 4.5 \times 10^{-4}$). Part a shows velocity profiles obtained with increasing S_t and four fixed M_t concentrations. Part b shows profiles with four fixed S_t concentrations and increasing M_t. In each figure the curved arrow shows the relative position of the ascending limbs obtained with higher fixed concentrations. To detetmine K_S, K_M, K_C, and V by the *isovelocity* method, points of equal velocity are chosen from each family of velocity profiles, as illustrated by the horizontal dashed lines at $v = 5$, 10, and 20 in Figure 3a,b. The isovelocity data are then plotted with M_t and S_t as the coordinate axes as shown in Figure 3c. The extrapolations from the asymptotically linear portion of the curves from the $S_t \gg M_t$ region intersect the abscissa near $-\bar{K}_S$ (eq 4b). These intercepts are replotted *vs.* the isovelocities (in the inset of Figure 3c) to obtain a more accurate determination of $\bar{K}_S$ (see text). The extrapolations from the asymptotically linear portion of the curves from the $M_t \gg S_t$ region intersect the ordinate near $-\bar{K}_M$ (eq 6b). In this case no replot of the intercepts is necessary.

Once K_S is determined, V and K_C are obtained from a plot of the slopes of the asymptotically linear portion of the isovelocity curves in the $S_t \gg M_t$ region *vs.* the reciprocal isovelocities (eq 5 and Figure 3d). K_C is obtained from the intercept on the ordinate, $1 - K_C\bar{K}_S$, and then V is obtained from the slope, $VK_C\bar{K}_S$. (In Figure 3d, with $\bar{K}_S = 1.3 \times 10^{-4}$, the estimations are $K_C = 1.00 \times 10^3$ and $V = 97$.) Similarly, K_C and V are also determined from the slopes of the asymptotically linear portion of the isovelocity curves in the $M_t \gg S_t$ region according to eq 7. (Figure 3e. With $\bar{K}_M = 4.5 \times 10^{-4}$, the estimations are $K_C = 1.02 \times 10^3$ and $V = 108$.) In these procedures the isovelocities from the $S_t \gg M_t$ and the $M_t \gg S_t$ regions need not be the same. To determine K_S, K_M, K_C, and V by the *fixed excess* method, the data are plotted in double-reciprocal form according to eq 4a or 6a, which are of the Michaelis–Menten form. In Figure 3f (fixed excess of S and eq 4a) the estimated maximal velocity is $V = 100$, and an apparent kinetic constant for each fixed excess, $\bar{K}_{C,app} = \bar{K}_C(1 + K_S(S_t - M_t))$, is determined from each slope. A plot of $\bar{K}_{C,app}$ *vs.* the fixed excess $S_t - M_t$ is shown in the inset of Figure 3f; K_C is determined from the intercept on the ordinate, and then K_S is found from the slope, or from the intercept on the abscissa. (The estimations are $K_C = 1.25 \times 10^3$ and $K_S = 8.3 \times 10^3$.) By analogy, for a fixed excess of M, the constants V, K_C, and K_M are determined using eq 6a and a replot of $\bar{K}_{C,app} = \bar{K}_C(1 + K_M(M_t - S_t))$ *vs.* $M_t - S_t$ (Figure 3g). (The estimations are $V = 100$, $K_C = 1.11 \times 10^3$, and $K_M = 2.22 \times 10^3$.) The loci of peak velocities (with M_t and S_t as coordinate axes) are shown in Figure 3h. The lower curve is the S_t locus (from profiles with fixed M_t and increasing S_t). The intersection on the abscissa, $\sqrt{\bar{K}_S\bar{K}_0}$, gives $K_0 = 7.36 \times 10^4$. The upper curve is the M_t locus (from profiles with fixed S_t and increasing M_t). The intersection on the ordinate, $\sqrt{\bar{K}_M\bar{K}_0}$, gives $K_0 = 6.26 \times 10^4$. The loci are not linear.

Special Features of Model I. If the velocity is studied with equimolar M_t and S_t, the profile lacks the qualitative features in Figure 2. The profile with equimolar M_t and S_t is always sigmoid, but this sigmoidicity is minimal and may only be apparent at concentrations in the region of $\bar{K}_0$ (Figure 4a). A double-reciprocal plot of the velocity with equimolar M_t and S_t *vs.* [$M_t = S_t$] is nonlinear, although it might appear linear in some regions (Figure 4b). Kinetic constants cannot be determined from the plot in the classic manner. As noted above, the peak velocity generally does not occur where $M_t = S_t$.

The peak velocities of the S_t profiles are shown in Figure 5. The curve does not pass through the origin, the intercept on the S_t axis being $S_t = \sqrt{\bar{K}_S\bar{K}_0}$. A double-reciprocal plot of Figure 5 is nonlinear, and kinetic constants cannot be determined from the plot in the classic manner.

If all but one of the parameters of the model are known, the remaining one can be found from eq 1 and 3 and any observation of the velocity. The advantage of determining K_0 from the locus of peak velocities is that the locus is independent of K_C and independent of V. The latter implies independence of the amount of active enzyme (or specific activity), which might vary in time.

Once K_0, K_C, K_S, and K_M are known, K_1 and K_2 can be calculated from the relations in Table I. A comparison of K_S and K_2 reveals the effect of M on the binding of S, and a comparison of K_M and K_1, the effect of S on the binding of M.

Model II

This is model I plus essential activation of the enzyme. The reactions are

$$\begin{array}{l} M + S \rightleftharpoons C \\ M + E \rightleftharpoons ME \end{array}$$

$$\begin{array}{ccccc} & & MEM & & \\ & {}^{+M}\!\!\diagup\!\!\diagdown & & \diagup\!\!\diagdown^{+S} & \\ ME & & \overset{+C}{\rightleftharpoons} & & MEC \longrightarrow ME + \text{products} \\ & {}_{+S}\diagdown\!\!\diagup & & \diagdown\!\!\diagup_{+M} & \\ & & MES & & \end{array}$$

If the model is studied in the region where $M_f \gg \bar{K}_A$, then all of the enzyme is activated, and model II reduces to model I.

The rate equation of model II is

$$\begin{aligned} v &= \frac{V'K_C'K_AM_fC}{K_AM_f[K_S'S_f + K_M'M_f + K_C'C + 1] + 1} \\ &= \frac{V'K_C'K_A(M_t - C)C}{K_A(M_t - C)[K_S'S_t + K_M'M_t + (K_C' - K_S' - K_M')C + 1] + 1} \end{aligned} \quad (9)$$

Since C can be obtained from eq 1, the initial velocity is again a function of two independent variables, M_t and S_t. A fruitful way to study the velocity surface is to examine profiles obtained by holding M_t or S_t fixed and increasing the other. Since M activates the enzyme, there is no symmetry between M_t and S_t.

The simulation of model II uses the same kinetic constants as model I (Figure 3, the lombricine kinase

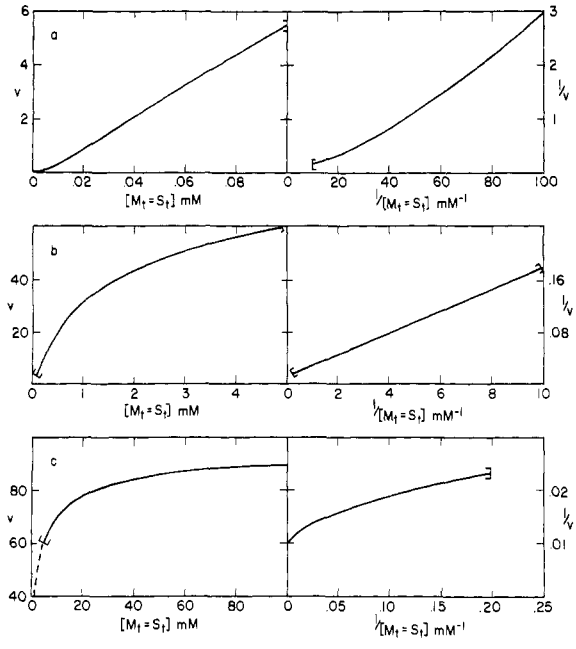

FIGURE 4: Model I: the velocity profile (and double-reciprocal plots) with equimolar M_t and S_t. The kinetic constants are the same as Figure 3. (a) The region 0–0.10 mM; (b) the region 0.10–5 mM; (c) the region 5–100 mM. Slight sigmoidicity is observed in the region of $\bar{K}_0$ = 0.014 mM. Double-reciprocal plots are not linear.

presented with model I. There is no analogy with model I in the region $S_t \gg M_t$, because with *the approximation of C*, $M_f \cong 0$, and all of the enzyme is assumed to be in the unmodified, inactive form.

Locus of Peak Velocities and Approximations of K_A. If $K_M' \neq 0$ the M_t profiles show a peak velocity. The S_t profiles always have a peak velocity (even if $K_S' = 0$),

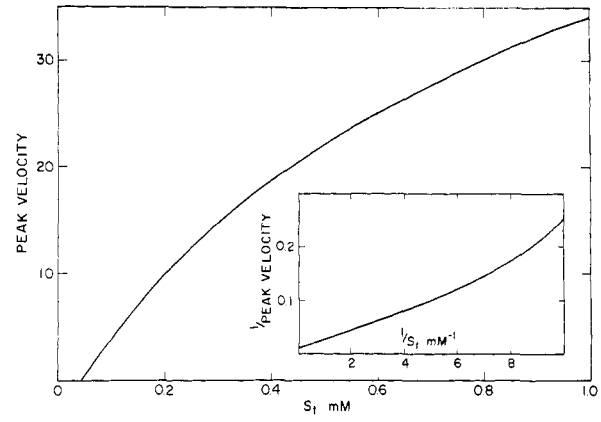

FIGURE 5: Model I: the velocity at the peak of the S_t profiles. The kinetic constants are the same as Figure 3. The intersection on the abscissa is $\sqrt{\bar{K}_S\bar{K}_0}$. The inset is a double-reciprocal plot.

data) plus $K_A = 5 \times 10^3$ M^{-1} to describe the M + E $\rightleftarrows$ ME reaction. Velocity profiles obtained with fixed M_t and increasing S_t (S_t profiles) are shown in Figure 6a. The profiles are similar to those of model I (Figure 3a), but the peak occurs at lower S_t concentrations and lower velocities. In model II the ascending limb may be concave or sigmoid, but unlike model I, there is no simple relation between the shape of the ascending limb and K_M' *vs.* K_C'. Inhibition by the ME + M $\rightleftarrows$ MEM reaction depresses the ascending limb of the profiles (downward arrow in Figure 6a). After the peak the velocity declines faster than in model I, because additional S_t both adds inhibitor (S) and removes activator (M).

M_t velocity profiles (obtained with fixed S_t and increasing M_t) are shown in Figure 6b. The profiles are similar to those of model I (Figure 3b) but the peaks are shifted to higher M_t concentrations and lower velocities. In model II the ascending limb is always sigmoid;[7] the profiles are more sigmoid than those of model I, because the addition of M_t both adds activator (M) and removes inhibitor (S). Inhibition by the ME + S $\rightleftarrows$ MES reaction depresses the ascending limb of the profiles (downward arrow in Figure 6b). When $M_t \gg S_t$ model II reduces to model I, and the corresponding profiles are superimposed. V', K_C', and K_M' can be determined from data obtained with $M_t \gg S_t$ by the isovelocity or fixed excess methods because as S_t is added at fixed M_t the enzyme is titrated from an activated to an unactivated form. The loci of the peaks are independent of V' and K_C'; they depend upon K_S', K_M', K_A, and K_0. (Equations describing the loci appear in the Appendix.)

The loci of the peak velocities for the simulation of model II are shown in Figure 6c. Both loci occur where M_t is greater than S_t (except the locus obtained from the S_t profiles at very low fixed M_t). In comparison with model I (Figure 3H), the loci are shifted such that M_t is even greater than S_t. Unlike model I the intersections of the loci on the axes cannot be simply expressed.

If K_0 is large relative to K_A, K_A may be estimated from the coordinates of the peak velocities. For peaks obtained from the S_t profiles and if the M_t concentration is large relative to $\bar{K}_0$, K_A is approximated by

$$K_A \cong \frac{(2S_t - M_t)}{(M_t - S_t)^2(K_M'M_t + 1)} \qquad (10)$$

Since K_A is positive, this equation implies that the locus occurs in the region $M_t \leq 2S_t$. For the locus obtained from the M_t profiles and if the S_t concentration is large relative to $\bar{K}_0$, K_A is approximated by

$$K_A \cong \frac{1}{K_M'(M_t - S_t)^2} \qquad (11)$$

If K_S' is large, these approximations of K_A are inaccurate. In the derivation of eq 10 and 11 the S_fK_S'

[7] The results concerning the shape of the ascending limb are based on the sign of the second derivative in a neighborhood of zero.

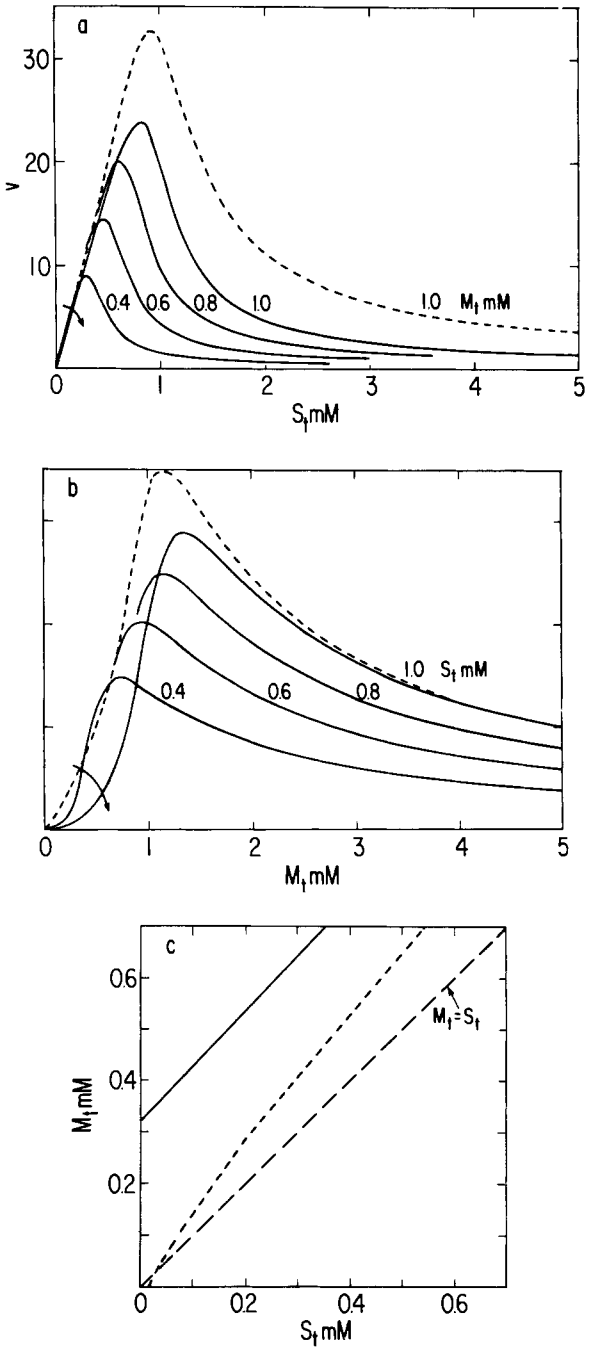

FIGURE 6: Simulation of model II. The parameters are the same as in Figure 3 plus $K_A = 5 \times 10^3$ ($\overline{K}_A = 2 \times 10^{-4}$). Part a shows velocity profiles obtained with fixed M_t and increasing S_t, and part b shows the profiles with fixed S_t and increasing M_t. For comparison, the dashed curve is the profile from Figure 3 (model I) with a fixed concentration of 1.0 mM. In each figure the curved arrow shows the relative position of the ascending limb of profiles obtained with higher fixed concentrations. Part c shows the loci of peak velocities. The lower curve is the locus from the S_t profiles, and the upper curve, the locus from the M_t profiles.

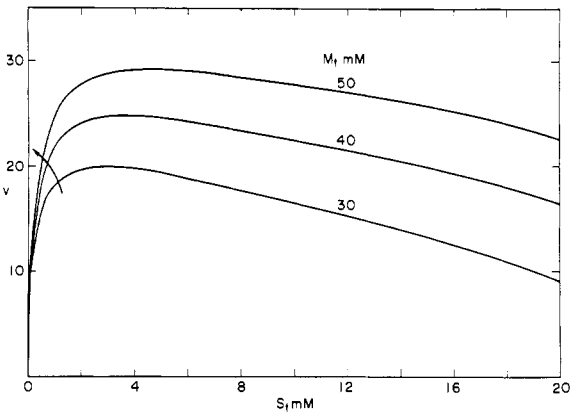

FIGURE 7: Model II: velocity profiles where the peak occurs at $M_t \gg S_t$. The kinetic constants are $V = 100$, $K_M' = 0$, $K_S' = 1 \times 10^6$, $K_C' = 1 \times 10^3$, $K_A = 1 \times 10^3$, and $K_0 = 1 \times 10^4$. Without inhibition from the ME + M $\rightleftarrows$ MEM reaction ($K_M' = 0$), the ascending limbs of profiles obtained with higher fixed M_t concentrations are shifted upward.

term is neglected relative to other terms in the rate equation, because *the approximation of C* assumes $S_f \cong 0$ ($M_t \gg S_t$). But if K_S' is large, $S_f K_S'$ may not be negligible. With the data in Figure 6c, where K_S' is at least three times larger than K_M' and K_C', the error in the estimation of K_A is about 25%.

In the S_t profiles, peak velocities in the region $M_t > 2S_t$ can occur, and they imply, relative to the other constants, a large K_S' and/or a small K_A. Figure 7 shows a simulation of model II where the peak in the S_t profiles occurs with M_t approximately ten times S_t. Here, K_S' is large (1×10^6) and K_A is small (1×10^3). A curve similar to the 50 mM profile in Figure 7 has been observed for ATP, Mg^{2+}, and glutamine synthetase (Hubbard and Stadtman, 1967).

Special Features of Model II. The velocity profile obtained with equimolar M_t and S_t is always sigmoid, but unlike model I this sigmoidicity is, in general, apparent at concentrations much greater than $\overline{K}_0$ (Figure 8).[8] The double-reciprocal plot of the velocity *vs.* [$S_t = M_t$] is not linear. As noted above, the peak velocity does not occur where $M_t = S_t$.

There appears to be no simple graphical method to obtain K_S' and K_0 or to estimate K_A in all cases.

The simplest case of model II is if only C combines with the activated enzyme ($K_S' = K_M' = 0$; this is also model III (see below) with $V = K_C = 0$). Figure 9 shows velocity profiles obtained with $M_t = S_t$ and with a fixed excess of M_t or S_t for this example of model II. The profile with $M_t = S_t$ is sigmoid and a fixed excess of S_t over M_t enhances the sigmoidicity. (Plots of $1/v$ *vs.* $1/[M_t = S_t]^2$ (not shown) are approximately linear.) With more M_t than S_t the profile appears hyperbolic. Similar profiles (and double-reciprocal plots) have been obtained with pyruvate carboxylase and interpreted as an allosteric mechanism with interacting sites on the enzyme for Mg^{2+}, ATP,

[8] This sigmoidicity has been observed, for example, with the pyrophosphatase from mouse liver cytoplasm (Horn *et al.*, 1967); it suggests that the enzyme, in addition to being inhibited by ATP, may be activated by Mg^{2+}

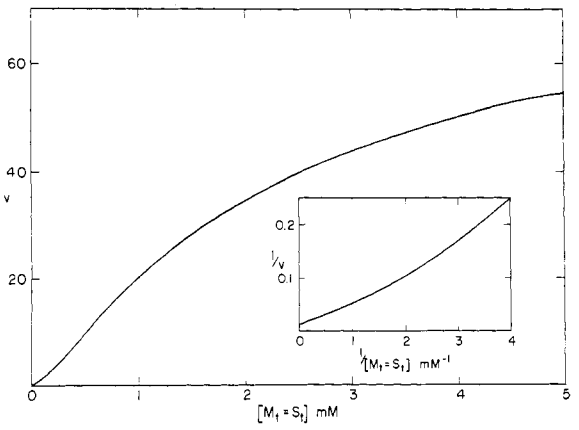

FIGURE 8: Model II: the velocity profile with equimolar M_t and S_t. The kinetic constants are the same as in Figure 6. Unlike model I (see Figure 4) sigmoidicity is observed at concentrations greater than $\overline{K}_0$ ($\overline{K}_0$ = 0.014 mM). The inset is a double-reciprocal plot.

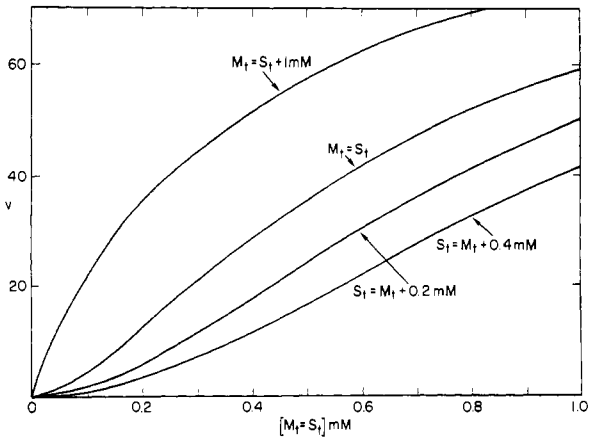

FIGURE 9: Model II: velocity profiles with $M_t = S_t$ and with a fixed excess of M_t or S_t. $K_S' = K_M' = 0$; $V' = 100$, $K_C' = 3.12 \times 10^3$, $K_A = 1 \times 10^4$, and $K_0 = 7.3 \times 10^4$. The kinetic constants are from Keech and Barritt (1967).

and Mg–ATP (Keech and Barritt, 1967). The profiles are, however, consistent with essential Mg^{2+} activation of an enzyme whose "active substrate" is the Mg–ATP complex.

Model III

This model assumes modification of the enzyme by M, and that C, but not S or M, reacts with the enzyme to form the final complexes. The reactions are

$$\begin{array}{ccccc} & & \mathrm{M} + \mathrm{S} \rightleftharpoons \mathrm{C} & & \\ & \overset{+\mathrm{C}}{} & & & \\ \mathrm{ME} & \rightleftharpoons & \mathrm{MEC} & \longrightarrow & \mathrm{ME} + \text{products} \\ {\scriptstyle +\mathrm{M}}\uparrow\downarrow & & {\scriptstyle +\mathrm{C}}\uparrow\downarrow{\scriptstyle +\mathrm{M}} & & \\ \mathrm{E} & \rightleftharpoons & \mathrm{EC} & \longrightarrow & \mathrm{E} + \text{products} \end{array}$$

The rate equation of the model is

$$v = \frac{(VK_C + V'K_C'K_AM_f)C}{K_AM_f(1 + K_C'C) + 1 + K_CC} = \frac{(VK_C + V'K_C'K_AM_t)C - V'K_C'K_AC^2}{1 + K_AM_t + (K_C + K_C'K_AM_t - K_A)C - K_C'K_AC^2} \quad (12)$$

The two paths of product formation are the distinctive characteristic of model III. If $V' = K_C' = 0$, (*i.e.*, ME is a dead-end complex) the model is model I with $K_S = 0$ (ME is replaced by EM, and K_A by K_M). If $V = K_C = 0$ (*i.e.*, E is inert) the model is a special case of model II ($K_S' = K_M' = 0$).

As in the previous models, the initial velocity is a function of two independent variables, M_t and S_t (since C can be obtained from eq 1). Again, a fruitful way to study the velocity surface is to examine profiles obtained by holding M_t or S_t fixed and increasing the other. Since the modifier but not the substrate combines with the enzyme, there is no symmetry between M_t and S_t.

In the simulation of model III we use hypothetical constants chosen so that the modified enzyme has twice the kinetic constant and twice the maximal velocity of the unmodified enzyme (Figure 10). The velocity profiles with fixed M_t and increasing S_t (S_t profiles, Figure 10a) are concave. In model III the S_t profiles are never sigmoid. In Figure 10a profiles obtained with higher fixed M_t concentrations are shifted upward, because the more M_t, the more activated enzyme. A peak in a velocity profile occurs because as S_t is added (at fixed M_t) the enzyme is titrated from an activated to an unactivated form. When $S_t \gg M_t$ the enzyme is entirely unactivated; with *the approximation of C*, eq 12 simplifies to

$$v = \frac{VM_t}{\overline{K}_C + M_t} \quad (13)$$

where v is the limiting velocity, independent of S_t at the fixed M_t. V and K_C can be determined graphically from the terminal portion of the three curves in Figure 10A and double-reciprocal plots of eq 13 (inset of Figure 10a). (If $V = 0$, there seems to be no simple way to determine K_C.)

Velocity profiles obtained with fixed S_t and increasing M_t (M_t profiles) are shown in Figure 10B. The ascending limb of profiles obtained with higher fixed S_t concentrations are shifted downward because the more S_t, the less activated enzyme. At low fixed S_t concentrations the profile appears concave throughout. At higher fixed S_t concentrations the profile is initially concave and then sigmoid. Initially $S_t \gg M_t$ and the reaction is catalyzed by the unactivated enzyme, which tends to saturate with C. As M_f increases, the enzyme becomes activated. The velocity increases rapidly because the activated enzyme has a greater maximal velocity than the unactivated enzyme ($V' = 100$ and $V = 50$). When $M_t \gg S_t$ the enzyme is entirely activated; with *the approximation of C*, eq 12 simplifies to

$$v = \frac{V'S_t}{\overline{K}_C' + S_t} \quad (14)$$

where v is the limiting velocity, independent of M_t at the fixed S_t. V' and K_C' can be determined graphically

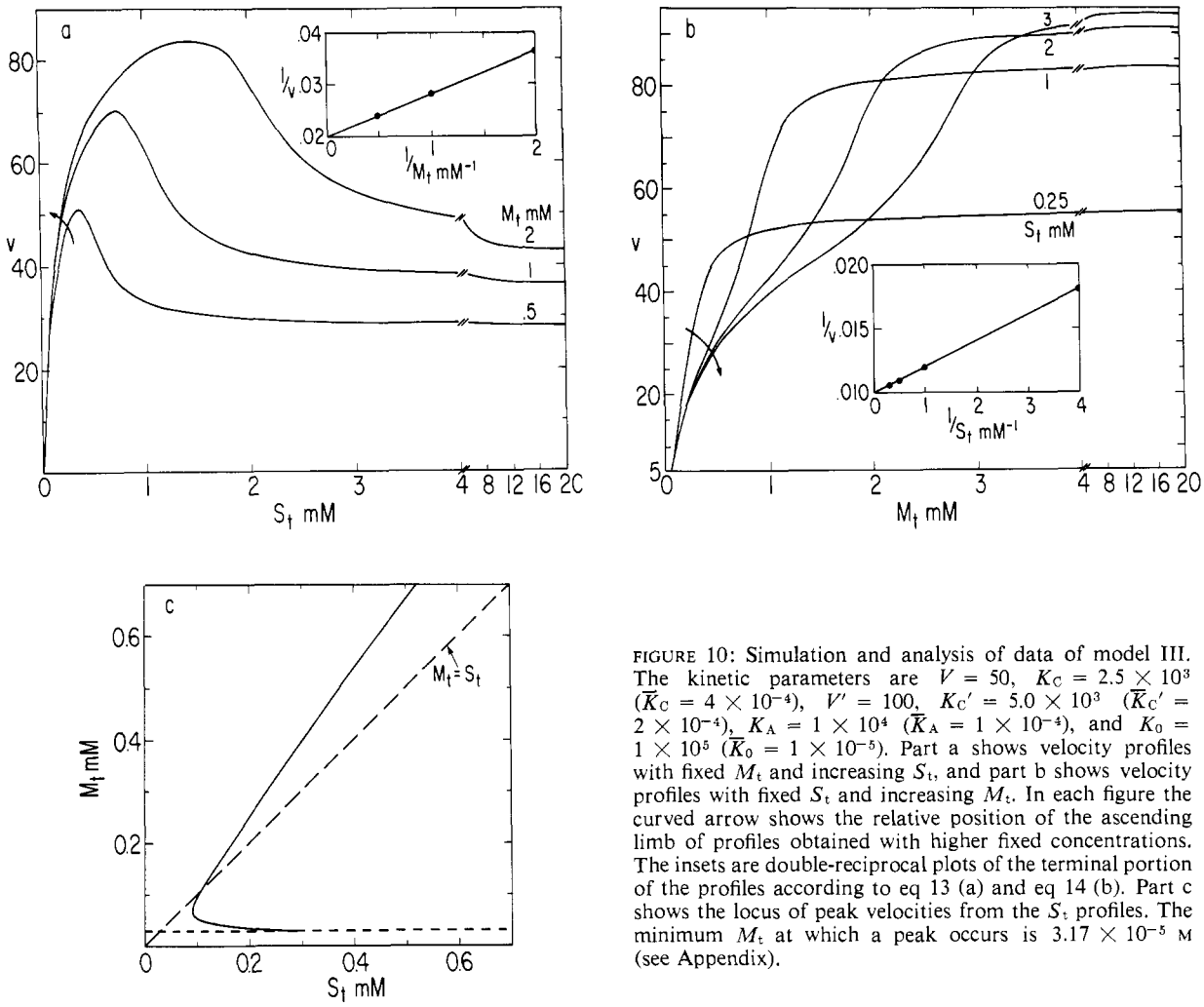

FIGURE 10: Simulation and analysis of data of model III. The kinetic parameters are $V = 50$, $K_C = 2.5 \times 10^3$ ($\bar{K}_C = 4 \times 10^{-4}$), $V' = 100$, $K_C' = 5.0 \times 10^3$ ($\bar{K}_C' = 2 \times 10^{-4}$), $K_A = 1 \times 10^4$ ($\bar{K}_A = 1 \times 10^{-4}$), and $K_0 = 1 \times 10^5$ ($\bar{K}_0 = 1 \times 10^{-5}$). Part a shows velocity profiles with fixed M_t and increasing S_t, and part b shows velocity profiles with fixed S_t and increasing M_t. In each figure the curved arrow shows the relative position of the ascending limb of profiles obtained with higher fixed concentrations. The insets are double-reciprocal plots of the terminal portion of the profiles according to eq 13 (a) and eq 14 (b). Part c shows the locus of peak velocities from the S_t profiles. The minimum M_t at which a peak occurs is 3.17×10^{-5} M (see Appendix).

from the terminal portion of the four curves in Figure 10b and double-reciprocal plots of eq 14 (inset of Figure 10b). (If $V' = 0$, there seems to be no simple way to determine K_C'.)

Kinetic constants different from those in the simulation produce velocity profiles different from those in Figure 10a,b. If V and K_A are small and S_t is large, the ascending limb of the M_t profiles may be sigmoid. If $V = 0$, the ascending limb is always sigmoid.[7] If the maximal velocity of the modified enzyme is less than that of the unmodified enzyme ($V' < V$), then the M_t profiles have a peak and the S_t profiles do not. Although the shapes of the two types of profiles depend upon the parameters, the terminal portion of the S_t profile reflects the unmodified enzyme, and the terminal portion of the M_t profiles reflect the modified enzyme.

Locus of Peak Velocities and Approximations of K_A. If $V' > V$, as in the simulation, the S_t profiles show a peak velocity (Figure 10a); the locus of the peak velocity is plotted in Figure 10c. Except at low fixed M_t concentrations the locus occurs where M_t exceeds S_t. With a smaller K_A, the locus would have been farther from the $M_t = S_t$ line. At high M_t concentrations the slope of the locus approaches unity, but at low M_t concentrations the locus crosses the $M_t = S_t$ line and asymptotically approaches an M_t value, the minimum M_t at which a peak occurs (see Appendix). The peak velocities at very low M_t concentrations may be difficult to observe.

Unlike the previous models the locus of the peak velocity depends upon all of the kinetic constants. If K_0 is large relative to K_A, K_A may be determined from individual peak velocities observed at M_t concentrations large relative to $\bar{K}_0$. Under these conditions K_A is approximated by

$$K_A \cong \frac{2S_t - M_t + \dfrac{K_C(1 - V/V')S_t^2 - (VK_C/V'K_C')M_t}{(S_t - M_t)^2}}{(S_t - M_t)^2} \quad (15)$$

where S_t and M_t are the coordinates of any peak velocity (see Appendix). If the unactivated enzyme is entirely inert (that is, $V = K_C = 0$), eq 15 reduces to

$$K_A \cong \frac{2S_t - M_t}{(S_t - M_t)^2} \quad (16)$$

In this case K_A can be found without knowledge of V' and K_C'. (Equation 16 is a simpler form of eq 10 because model III with $V = K_C = 0$ is model II with $K_S' = K_M' = 0$.) Since K_A is positive, eq 16 implies

that each peak velocity occurs in the region $M_t \leq 2S_t$; in the same way, eq 15 suggests that the peaks occur in the region: $M_t \leq (2 + K_C S_t)S_t$. These equations are approximations of K_A when $K_0 \gg K_A$ and $M_t \gg \bar{K}_0$. From the locus of peak velocities in Figure 10c, with M_t in the range 2–8 mM, K_A was estimated to within 10%.

Special Features of Model III. The initial portion of the velocity profile with equimolar M_t and S_t is always sigmoid, and like model I, the slight sigmoidicity may only be apparent at concentrations in the region of $\bar{K}_0$. The velocity with $M_t = S_t$ eventually approaches V'.

Once V, V', K_C, K_C', and K_A are determined, a crude estimate of K_0 can be obtained from eq 1 and 12 by calculating C in eq 12 at any velocity and then calculating K_0 from eq 1.

Conclusions

The kinetic model described here provides a framework for studying and devising hypotheses about an enzyme reaction in which a modifier and a reactant combine with the enzyme and with each other. The modifier's dual role, combination with both the enzyme and a reactant, produces a variety of complex kinetic curves. For example, sigmoid velocity curves can occur in this model, which does not assume an enzyme with multiple interacting subunits.

The general model (Figure 1 and eq 1 and 2) has three disadvantages. First, it may not be the simplest model that is consistent with the data. Second, it requires ten independent parameters, whereas the special cases require at most six. (A statistical fitting of the data to the general model probably would not determine the parameters to an acceptable degree of certainty.) Third, the three special cases allow simple graphical estimations of many kinetic parameters. Thus, distinctions among models I–III are important.

Qualitative criteria for distinguishing the special cases are: (1) sigmoidicity or concavity of the ascending limb of a velocity profile, (2) the relative position of profiles obtained with higher fixed concentrations of modifier or reactant, and (3) the presence of a peak velocity. Because these criteria depend upon individual parameters, they may also be used as tests of consistency. For example, in model I the absence of a peak in the M_t profile (implying $K_M = 0$) and a sigmoid ascending limb in the S_t profile (implying $K_M > K_C$) are inconsistent. (4) The position of the peak velocity; in general, the peak velocities occur nearest the equimolar ratio of M_t to S_t in model I (Figure 3h), in the region $M_t \leq 2S_t$ in model III (Figure 10c), and farthest from the equimolar ratio in model II (Figure 6c). Indeed, peak velocities in the region where M_t greatly exceeds S_t suggest simultaneous activation by M and inhibition by S (Figure 7). (5) Sigmoidicity of the velocity profile with equimolar M_t and S_t; in model II the velocity profile with $M_t = S_t$ is sigmoid at concentrations much greater than $\bar{K}_0$, but in model I, only at concentrations in the range of $\bar{K}_0$, which can be quite low, is the profile sigmoid (Figure 4 *vs.* Figure 8). Criteria 4 and 5 may be difficult to apply with ADP and other nucleotides that have a relatively low affinity for divalent cations (small K_0); (6) the velocity with excess modifier or reactant. The two paths of product formation, evident as constant velocities in the terminal portions of the S_t and M_t profiles, are the distinctive feature of model III (Figure 10). If $V = K_C = 0$, model III is a special case of model II (with $K_S' = K_M' = 0$); if $V' = K_C' = 0$, model III is a special case of model I (with $K_S = 0$ and K_A replaced by K_M).

A difficult distinction is between model I and model II, which is tantamount to discerning activation by free modifier in the presence of inhibition by free substrate. Here, criteria 4 and 5 are particularly useful. If the concentration of free modifier greatly exceeds $\bar{K}_A$, all of the enzyme is modified, and model II reduces to model I.

None of the criteria alone distinguishes one model from the other, but together, they are heuristics to that end. Of course, the data may be statistically fitted to any of the models, and presumably the appropriate model would have the best fit. General-purpose computer programs are available for statistically fitting data to nonlinear models (Berman and Weiss, 1967).

The graphical methods for determining the parameters of the models are presented as (a) simple, rapid ways to estimate the constants without resort to elaborate statistical procedures, and (b) methods to obtain initial estimates of the parameters if the data are to be fitted statistically to the appropriate model and equations. The procedures do not require the association constant of the modifier–reactant complex, K_0; in some cases that constant can be estimated graphically from the enzyme kinetic data. Of course, K_0 and some of the other association constants can also be determined by physical methods independent of the enzymatic reaction.

The advantages of studying the velocity surface primarily by profiles obtained with one variable (M_t or S_t) fixed and the other increased are (1) different effects of the modifier and reactant can be distinguished, and (2) several parameters can be estimated graphically. Although equal concentrations of modifier and reactant tend to minimize inhibition by both free species, the peak velocity does not occur when $M_t = S_t$; also the velocity profile with $M_t = S_t$ is always sigmoid (Figure 2 *vs.* Figure 4, for example). Since double-reciprocal plots of the velocity *vs.* $[M_t = S_t]$ are nonlinear (Figures 4 and 8), kinetic constants cannot be determined from these plots in the classic manner.

Acknowledgment

We thank Drs. John Z. Hearon and Earl R. Stadtman and members of their groups for several helpful discussions.

Appendix

Model I (Profiles with fixed M_t and increasing S_t)

(1) The ascending limb is concave even though $K_M > K_C$ if M_t is less than the positive root of

$$(K_M - K_C)M_t^2 - (K_S + K_C)\bar{K}_0 M_t - \bar{K}_0(K_S\bar{K}_0 + 1) = 0 \quad \text{(A-1)}$$

(2) The locus of peak velocities is

$$(Q - \bar{K}_0)S_t^2 - 2M_tQS_t + Q[(M_t + \bar{K}_0)^2 - \bar{K}_0Q] = 0 \quad \text{(A-2)}$$

where $Q = \bar{K}_S(K_M M_t + 1)$. The larger root is chosen if $Q > M_t + \bar{K}_0$, and the smaller root is chosen if $M_t + \bar{K}_0 > Q$. If $M_t + \bar{K}_0 = Q$, eq A-2 is replaced by $S_t = Q$. The locus of peak velocities is nonlinear, and more curvature is evident if K_0 is small or if K_M/K_S is near unity. At high M_t and S_t concentrations, the locus is asymptotically linear with a slope of unity. If $K_M = 0$ the locus of peak velocities is linear

$$S_t = [M_t(\bar{K}_S - (\bar{K}_S\bar{K}_0)^{1/2})/(\bar{K}_S - \bar{K}_0)] + (\bar{K}_S\bar{K}_0)^{1/2} \quad (K_S \neq K_0) \quad \text{(A-3)}$$

$$S_t = M_t/2 + \bar{K}_0 \quad (K_S = K_0) \quad \text{(A-4)}$$

If $K_S = K_M$ the peak occurs when the variable that is being increased is in excess. The smaller K_0, the larger the excess.

Analogous results for the profiles with fixed S_t and increasing M_t are obtained by replacing K_S by K_M and S_t by M_t.

Model II

(1) The locus of peak velocities obtained with fixed M_t and increasing S_t is

$$(Q - \bar{K}_0)(\bar{K}_S\bar{K}_A + \bar{K}_0M_t)S_t^2 - 2\{Q\bar{K}_0M_t^2 + \bar{K}_A\bar{K}_S(\bar{K}_A\bar{K}_S + M_t(Q + \bar{K}_0))\}S_t + (\bar{K}_S\bar{K}_A + M_tQ)\{\bar{K}_A\bar{K}_S(M_t + 2\bar{K}_0) + \bar{K}_0[(M_t + \bar{K}_0)^2 - \bar{K}_0Q]\} = 0 \quad \text{(A-5)}$$

where $Q = \bar{K}_S'(\bar{K}_M'M_t + 1)$. In general, the smaller root is chosen.

(2) The locus of peak velocities obtained with fixed S_t and increasing M_t is

$$[\bar{K}_A\bar{K}_M' + \bar{K}_0(\bar{K}_0 - Q)]M_t^3 + [(S_t + \bar{K}_0)^2 - Q\bar{K}_0 - 4\bar{K}_A\bar{K}_M']S_tM_t^2 + [6S_t(S_t + \bar{K}_0)\bar{K}_M'\bar{K}_A - \{(S_t + \bar{K}_0)^2 + \bar{K}_A\bar{K}_M' - Q\bar{K}_0\}\{\bar{K}_A\bar{K}_M' + Q\bar{K}_0\}]M_t + 2\bar{K}_A\bar{K}_M'[2\bar{K}_A\bar{K}_M'S_t - (S_t + \bar{K}_0) \times (\bar{K}_A\bar{K}_M' + (S_t + \bar{K}_0)^2 - Q\bar{K}_0)] = 0 \quad \text{(A-6)}$$

where $Q = K_M'(\bar{K}_S'S_t + 1)$. The roots of this cubic equation have not been investigated.

Model III

(1) The minimum M_t at which a peak occurs is the positive root of

$$(V' - V)M_t^2 + (V'\bar{K}_C - V\bar{K}_C')M_t - V\bar{K}_C'\bar{K}_A = 0 \quad \text{(A-7)}$$

If $V = K_C = 0$, the minimum M_t at which a peak occurs is zero.

(2) Equation 15 is based on *the approximation of C* ($S_t \ll M_t$); it also assumes $V'K_C' \gg VK_C$, that is, the unmodified enzyme has little activity. An equation analogous to eq 15 but without this latter assumption is

$$\frac{VK_C}{V'K_C'}\bar{K}_A^2 + \left[M_t - 2S_t + K_C(V/V' - 1)S_t^2 + \frac{VK_C}{V'K_C'}M_t\right] \times \bar{K}_A + (S_t - M_t)^2 = 0 \quad \text{(A-8)}$$

$\bar{K}_A$ is the smaller root of this equation.

References

Atkinson, D. E., Hathaway, J. A., and Smith, E. C. (1965), *J. Biol. Chem. 240*, 2682.

Beck, W. S. (1967), *J. Biol. Chem. 242*, 3148.

Berman, M., and Weiss, M. F. (1967), Users Manual for SAAM (Simulation, Analysis and Modeling), Public Health Service Publication No. 1703, Washington, D. C., Superintendent of Documents, U. S. Government Printing Office.

Cleland, W. W. (1963), *Biochim. Biophys. Acta 67*, 173.

Cleland, W. W. (1967), *Ann. Rev. Biochem. 36*, 77.

Frieden, C. (1964), *J. Biol. Chem. 239*, 3522.

Gaffney, J. J., and O'Sullivan, W. J. (1964), *Biochem. J. 90*, 177.

Gulbinsky, J. S., and Cleland, W. W. (1968), *Biochemistry 7*, 566.

Horn, A., Börnig, H., and Thiele, G. (1967), *European J. Biochem. 2*, 243.

Hubbard, J. S., and Stadtman, E. R. (1967), *J. Bacteriol. 94*, 1007.

Keech, B., and Barritt, G. J. (1967), *J. Biol. Chem. 242*, 1983.

London, W. P. (1968), *Bull. Math. Biophys. 30*, 253.

Mildvan, A. S., and Cohn, M. (1966), *J. Biol. Chem. 241*, 1178.

Morrison, J. F., and James, E. (1965), *Biochem. J. 97*, 37.

Morrison, J. F., O'Sullivan, W. J., and Ogston, A. G. (1961), *Biochim. Biophys. Acta 52*, 82.

Schramm, V. L., and Morrison, J. F. (1968), *Biochemistry 7*, 3642.

Steck, T. L., Caicuts, M. J., and Wilson, R. G. (1968), *J. Biol. Chem. 243*, 2769.